Measuring the weak mixing angle at SBND

CETUP* Workshop, South Dakota

Antonio Ferreira

in collaboration with
Gustavo Alves,
Shirley Li,
Pedro Machado and
Yuber Perez

Instituto de Física da Universidade de São Paulo

June 13, 2023

FAPESP

Outline

1. Measuring $\sin^2\theta_W$
2. The SBND detector
3. Our analysis
4. Signal and background
5. Conclusions
6. References

We propose a new measurement of the weak mixing angle using neutrino - electron scattering events at FERMILAB's new short baseline liquid Argon time projection chamber detector.

Combining gauge fields

B ($U(1)_Y$) and W^3 ($SU(2)_L$) combine to form the

$$B = \cos\theta_W A - \sin\theta_W Z$$
$$W^3 = \sin\theta_W A + \cos\theta_W Z$$

Combining gauge fields

B ($U(1)_Y$) and W^3 ($SU(2)_L$) combine to form the

$$B = \cos\theta_W A - \sin\theta_W Z$$
$$W^3 = \sin\theta_W A + \cos\theta_W Z$$

$$\mathcal{L} = -\frac{g}{\sqrt{2}}\overline{\psi}\gamma^\mu\left(W^\pm_\mu T^\pm + \sqrt{2}W^3_\mu T^3\right)\psi - g'\overline{\psi}\gamma^\mu B_\mu Y\psi$$

$$\downarrow$$

$$\mathcal{L} = -\frac{g}{\sqrt{2}}\overline{\psi}\gamma^\mu W^\pm_\mu T^\pm\psi - e\overline{\psi}\gamma^\mu A_\mu Q\psi - e\overline{\psi}\gamma^\mu(gc_W T^3 - g's_W Y)Z_\mu\psi$$

Combining gauge fields

B ($U(1)_Y$) and W^3 ($SU(2)_L$) combine to form the

$$B = \cos\theta_W A - \sin\theta_W Z$$
$$W^3 = \sin\theta_W A + \cos\theta_W Z$$

$$\tan\theta_W = \frac{g'}{g} \quad e = \frac{gg'}{\sqrt{g^2 + g'^2}}$$

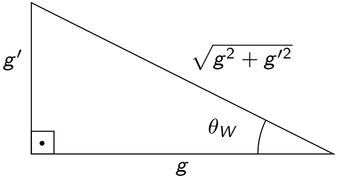

Combining gauge fields

B ($U(1)_Y$) and W^3 ($SU(2)_L$) combine to form the

$$B = \cos\theta_W A - \sin\theta_W Z$$
$$W^3 = \sin\theta_W A + \cos\theta_W Z$$

Symmetry breaking and masses

$$D_\mu = \partial_\mu + igW_\mu^a T^a + ig' B_\mu Y_H \,,$$

gauge bosons get their masses from

$$|D_\mu H|^2 \,.$$

$$\tan\theta_W = \frac{g'}{g} \qquad e = \frac{gg'}{\sqrt{g^2 + g'^2}}$$

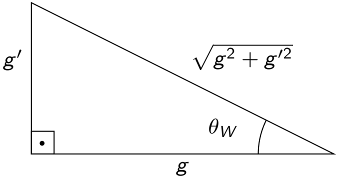

Combining gauge fields

B ($U(1)_Y$) and W^3 ($SU(2)_L$) combine to form the

$$B = \cos\theta_W A - \sin\theta_W Z$$
$$W^3 = \sin\theta_W A + \cos\theta_W Z$$

Symmetry breaking and masses

$$D_\mu = \partial_\mu + igW_\mu^a T^a + ig' B_\mu Y_H \,,$$

gauge bosons get their masses from

$$|D_\mu H|^2 \,.$$

$$\tan\theta_W = \frac{g'}{g} \quad e = \frac{gg'}{\sqrt{g^2 + g'^2}}$$

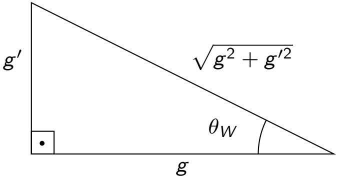

$$m_W^2 = \frac{g^2 v^2}{2} \quad m_Z^2 = \frac{(g^2 + g'^2)v^2}{2} \,,$$

Combining gauge fields

B ($U(1)_Y$) and W^3 ($SU(2)_L$) combine to form the

$$B = \cos\theta_W A - \sin\theta_W Z$$
$$W^3 = \sin\theta_W A + \cos\theta_W Z$$

$$\tan\theta_W = \frac{g'}{g} \quad e = \frac{gg'}{\sqrt{g^2 + g'^2}}$$

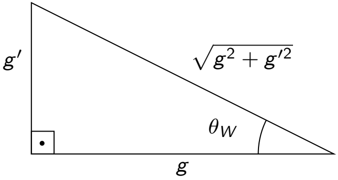

Symmetry breaking and masses

$$D_\mu = \partial_\mu + igW_\mu^a T^a + ig' B_\mu Y_H \,,$$

gauge bosons get their masses from

$$|D_\mu H|^2 \,.$$

$$m_W^2 = \frac{g^2 v^2}{2} \quad m_Z^2 = \frac{(g^2 + g'^2)v^2}{2} \,,$$

So using the previous result

$$\sin^2\theta_W = 1 - \frac{m_W^2}{m_Z^2} \,.$$

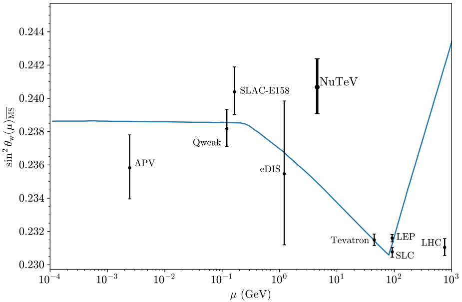

Data points from [T+18].

- Different measurements using different techniques were performed to determine $\sin^2\theta_W$.

Past measurements of $\sin^2\theta_W$

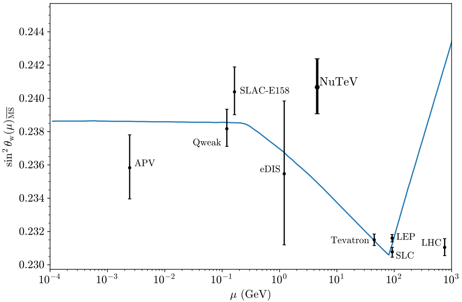

Data points from [T+18].

- Different measurements using different techniques were performed to determine $\sin^2\theta_W$.
- Only one measurement was performed using neutrinos, and it the one with the biggest disagreement with the Standard Model prediction.

Past measurements of $\sin^2\theta_W$

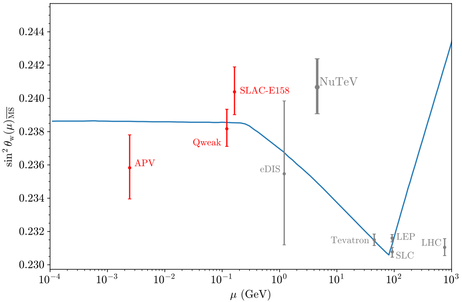

Data points from [T+18].

Low energy measurements

- **APV:** Measurements of PV effects of highly suppressed atomic transitions. Most precise measurement is performed using ^{133}Cs [WBC+97].
- **Qweak:** Performed at JLab, polarized electron beam scatters off protons. Measuring the proton's weak charge $Q_w^p = 1 - 4\sin^2\theta_W$ using polarization asymmetry in the cross section, one can extract $\sin^2\theta_W$.
- **SLAC-158:** Møller scattering measurement experiment at SLAC, using polarized electrons. $Q_w^e = -1 + 4\sin^2\theta_W$ is extracted using the polarization asymmetry of the cross section.

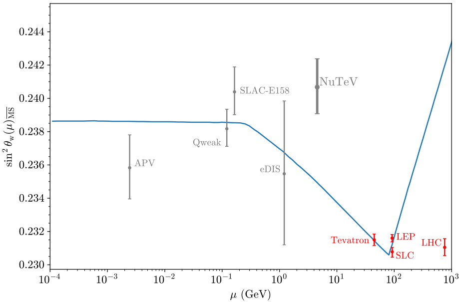

Data points from [T+18].

Collider searches

- Mostly conducted at the m_Z pole.
- Exploits the forward-backward asymmetry induced by the vector and axial-vector electroweak couplings that contain the weak mixing angle.
- Most precise measurements to date, at the 0.1% level.

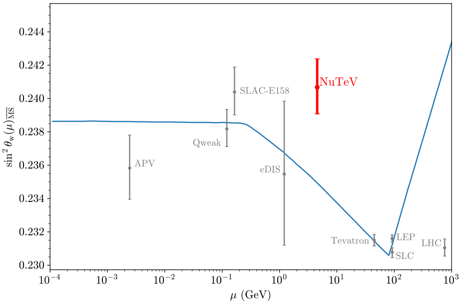

Data points from [T+18].

NuTeV

- Neutrino DIS experiment performed at Fermilab, using a 800 GeV proton beam from the Tevatron ring.
- Steel scintillator target, composed primarily of isoscalar particles.
- The nature of the target allows for a simple relation for the NC-CC cross section ratio, which cancels uncertainties.
- Disagreement with the Standard Model prediction (given other measurements).

- The statistics of neutrino - electron scattering events in SBND's LArTPC and some properties of the detector (PRISM) point for a promising measure.

- The statistics of neutrino - electron scattering events in SBND's LArTPC and some properties of the detector (PRISM) point for a promising measure.
- Past measurement of $\sin^2\theta_W$ using neutrino physics (NuTEV) is in tension with other experiments.

- The statistics of neutrino - electron scattering events in SBND's LArTPC and some properties of the detector (PRISM) point for a promising measure.
- Past measurement of $\sin^2\theta_W$ using neutrino physics (NuTEV) is in tension with other experiments.
- SBND will rely on neutrino - electron measurements to measure its flux, and this process is sensitive to $\sin^2\theta_W$.

- The statistics of neutrino - electron scattering events in SBND's LArTPC and some properties of the detector (PRISM) point for a promising measure.
- Past measurement of $\sin^2\theta_W$ using neutrino physics (NuTEV) is in tension with other experiments.
- SBND will rely on neutrino - electron measurements to measure its flux, and this process is sensitive to $\sin^2\theta_W$.
- Access the robustness of this measurement in the presence of new Physics scenarios.

In the literature the sensitivity of neutrino - electron scattering experiments to radiative corrections is debated (e.g. [BKS95, MMGM21]).

On-shell renormalization scheme

No scale dependence on the weak mixing angle:

$$\sin^2\theta_W = 1 - \frac{m_W^2}{m_Z^2}\,.$$

In the literature the sensitivity of neutrino - electron scattering experiments to radiative corrections is debated (e.g. [BKS95, MMGM21]).

On-shell renormalization scheme

No scale dependence on the weak mixing angle:

$$\sin^2\theta_W = 1 - \frac{m_W^2}{m_Z^2}\,.$$

$\overline{\text{MS}}$ renormalization scheme

Physical observable is the (process dependent) combination

$$\hat{\kappa}(q^2)\sin^2\hat{\theta}_W(m_Z)\,,$$

In the literature the sensitivity of neutrino - electron scattering experiments to radiative corrections is debated (e.g. [BKS95, MMGM21]).

On-shell renormalization scheme

No scale dependence on the weak mixing angle:

$$\sin^2\theta_W = 1 - \frac{m_W^2}{m_Z^2}\,.$$

$\overline{\text{MS}}$ renormalization scheme

Physical observable is the (process dependent) combination

$$\hat{\kappa}(q^2)\sin^2\hat{\theta}_W(m_Z)\,,$$

κ factor definition

κ is a process dependent form factor arising from electroweak corrections [FOS04],

$$\hat{\kappa}(q^2) = 1 - \frac{\alpha}{2\pi\sin^2\hat{\theta}_W}\left(\sum_f 2Q_f(T_f^3 - 2\sin^2\hat{\theta}_W Q_f)(\dots) + \dots\right)\,,$$

In the literature the sensitivity of neutrino - electron scattering experiments to radiative corrections is debated (e.g. [BKS95, MMGM21]).

On-shell renormalization scheme

No scale dependence on the weak mixing angle:

$$\sin^2\theta_W = 1 - \frac{m_W^2}{m_Z^2}\,.$$

$\overline{\text{MS}}$ renormalization scheme

Physical observable is the (process dependent) combination

$$\hat{\kappa}(q^2)\sin^2\hat{\theta}_W(m_Z)\,,$$

κ factor definition

κ is a process dependent form factor arising from electroweak corrections [FOS04],

$$\hat{\kappa}(q^2) = 1 - \frac{\alpha}{2\pi\sin^2\hat{\theta}_W}\left(\sum_f 2Q_f(T_f^3 - 2\sin^2\hat{\theta}_W Q_f)(\dots) + \dots\right)\,,$$

At low q^2 the light quark contribution to the $\gamma - Z$ vacuum polarization becomes nonperturbative, so a data driven analysis must be performed [KMMS13]

$$\frac{1}{3}\sum_f Q_f(T_f^3 - 2\sin^2\hat{\theta}_W Q_f)\log\frac{m_f^2}{m_Z^2} \longrightarrow -6.88 \pm 0.06\,.$$

Cross section

The one loop neutrino - electron scattering cross section reads

$$\frac{d\sigma}{dT} = \frac{2m_e G_F^2}{\pi}\left(g_L^2(T)\left(1+\frac{\alpha}{\pi}f_-(z)\right)+g_R^2(T)\left(1+\frac{\alpha}{\pi}f_+(z)\right)\left(1-\frac{T}{E_\nu}\right)^2+g_L(T)g_R(T)\left(1+\frac{\alpha}{\pi}f_{+-}(z)\right)\right),$$

where $z = T/E_\nu$, $g_R(T) = \rho_{NC}(1/2 - \kappa_{\nu_l}(T)\sin\hat{\theta}_W(\mu))$ and $g_L(T) = -\rho_{NC}\kappa_{\nu_l}(T)\sin\hat{\theta}_W(\mu)$.

Cross section

The one loop neutrino - electron scattering cross section reads

$$\frac{d\sigma}{dT} = \frac{2m_e G_F^2}{\pi}\left(g_L^2(T)\left(1+\frac{\alpha}{\pi}f_-(z)\right) + g_R^2(T)\left(1+\frac{\alpha}{\pi}f_+(z)\right)\left(1-\frac{T}{E_\nu}\right)^2 + g_L(T)g_R(T)\left(1+\frac{\alpha}{\pi}f_{+-}(z)\right)\right),$$

where $z = T/E_\nu$, $g_R(T) = \rho_{NC}(1/2 - \kappa_{\nu_l}(T)\sin\hat{\theta}_W(\mu))$ and $g_L(T) = -\rho_{NC}\kappa_{\nu_l}(T)\sin\hat{\theta}_W(\mu)$.

The $g_R(T)$ and $g_L(T)$ factor account for electroweak corrections, for example:

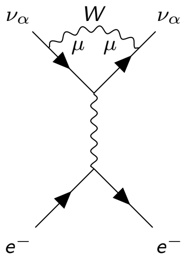

Cross section

The one loop neutrino - electron scattering cross section reads

$$\frac{d\sigma}{dT} = \frac{2m_e G_F^2}{\pi}\left(g_L^2(T)\left(1+\frac{\alpha}{\pi}f_-(z)\right) + g_R^2(T)\left(1+\frac{\alpha}{\pi}f_+(z)\right)\left(1-\frac{T}{E_\nu}\right)^2 + g_L(T)g_R(T)\left(1+\frac{\alpha}{\pi}f_{+-}(z)\right)\right),$$

where $z = T/E_\nu$, $g_R(T) = \rho_{NC}(1/2 - \kappa_{\nu_l}(T)\sin\hat{\theta}_W(\mu))$ and $g_L(T) = -\rho_{NC}\kappa_{\nu_l}(T)\sin\hat{\theta}_W(\mu)$.

The $f_-(z)$, $f_+(z)$ and $f_{+-}(z)$ factors account for QED corrections, for example:

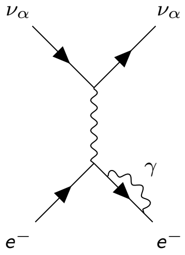

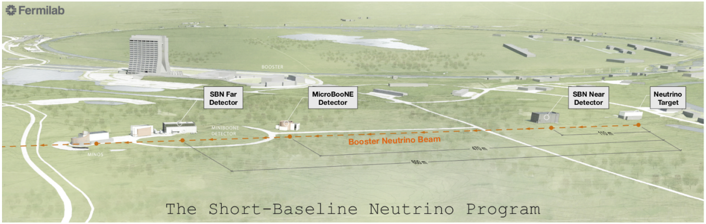

[MPS19].

- The first detector downstream Fermilab's Booster neutrino beam.

The SBND detector

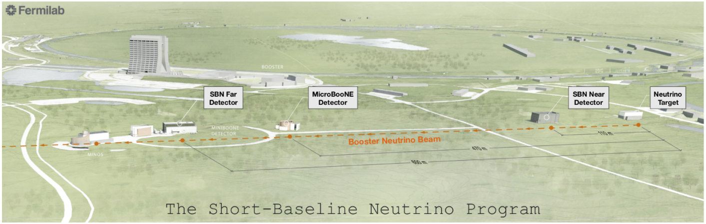

[MPS19].

- The first detector downstream Fermilab's Booster neutrino beam.
- State of the art liquid Argon Time Projection Chamber (LArTPC).

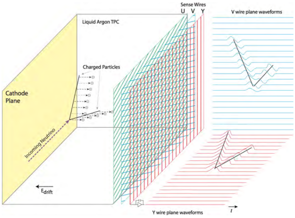

[A^+19]

The SBND detector

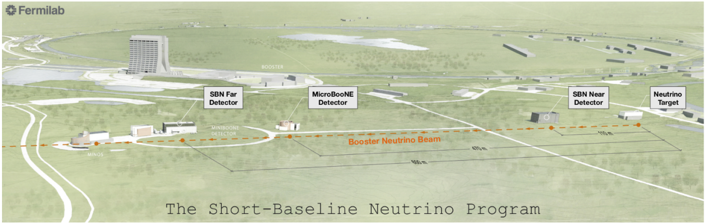

[MPS19].

- The first detector downstream Fermilab's Booster neutrino beam.
- State of the art liquid Argon Time Projection Chamber (LArTPC).

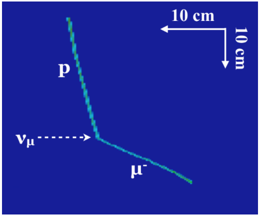

[A+19]

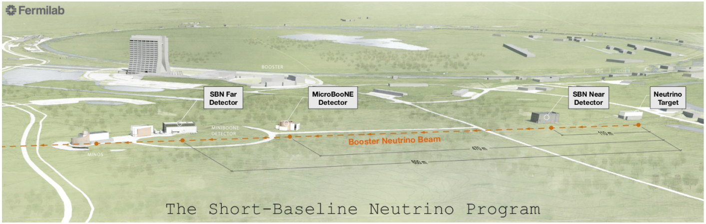

[MPS19].

- The first detector downstream Fermilab's Booster neutrino beam.
- State of the art liquid Argon Time Projection Chamber (LArTPC).
- Main physics goals include the measurement of the flux of the neutrino beam at a near detector, search for new physics (heavy neutral leptons) and test the technology to be deployed at DUNE.

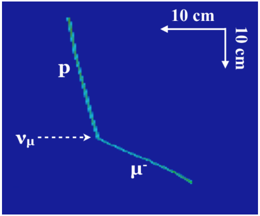

[A+19]

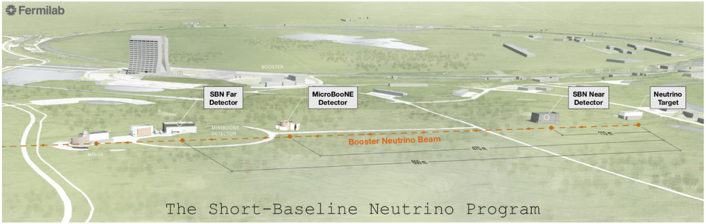

[MPS19].

- The first detector downstream Fermilab's Booster neutrino beam.
- State of the art liquid Argon Time Projection Chamber (LArTPC).
- Main physics goals include the measurement of the flux of the neutrino beam at a near detector, search for new physics (heavy neutral leptons) and test the technology to be deployed at DUNE.
- Data taking is expected to be begin late 2023 / early 2024.

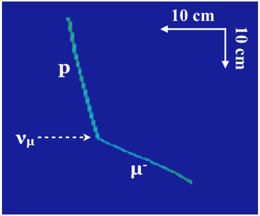

[A$^+$19]

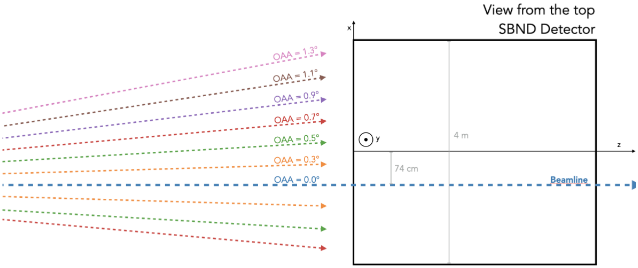

[TP21]

- The SBND detector is positioned very close to the proton target ($\sim$ 100 m).

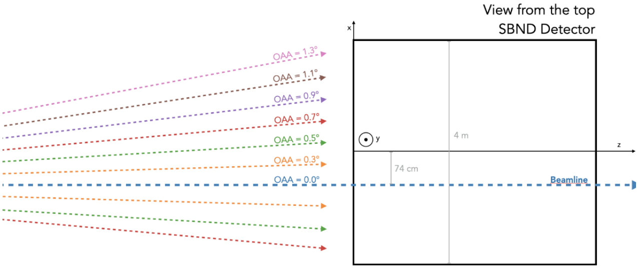

[TP21]

- The SBND detector is positioned very close to the proton target ($\sim$ 100 m).
- Different neutrino production channels result in different beam spectra and composition as one moves off-axis.

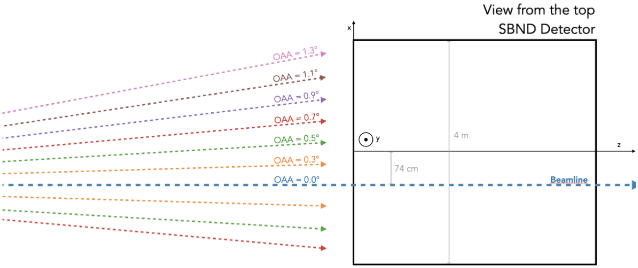

[TP21]

- The SBND detector is positioned very close to the proton target ($\sim$ 100 m).
- Different neutrino production channels result in different beam spectra and composition as one moves off-axis.
- The event position reconstruction capabilities of SBND allows this difference to be exploited.

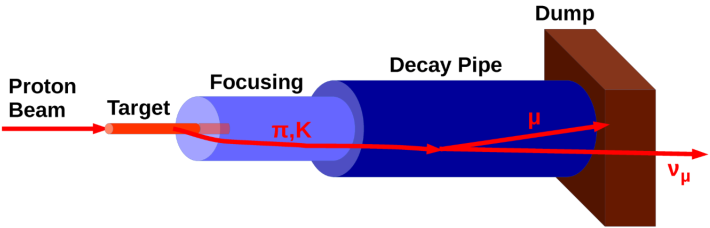

[DLL19].

Rough estimate of the flux

The flux

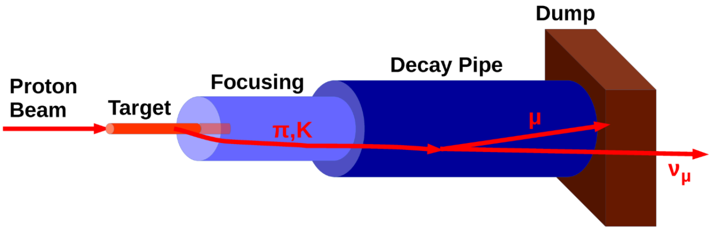

[DLL19].

Rough estimate of the flux

- A 8 GeV proton beam hits a target at rest, producing multiple hadrons.
  $\rightarrow$ Simulation of proton - proton collisions with Pythia, to get $\pi^\pm$ and $\pi^\pm$ $K^\pm$.

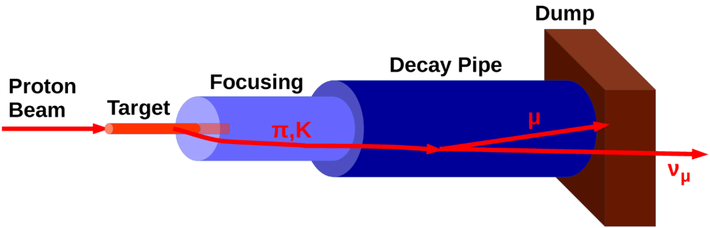

[DLL19].

Rough estimate of the flux

- A 8 GeV proton beam hits a target at rest, producing multiple hadrons.
$\rightarrow$ Simulation of proton - proton collisions with Pythia, to get $\pi^{\pm}$ and $\pi^{\pm}$ $K^{\pm}$.
- Positively charged particles are focused and negatively charged particles deflected.
$\rightarrow$ Alignment of π^{+} and K^{+} with the beam direction, with 10% forward K^{-} and π^{-} contamination.

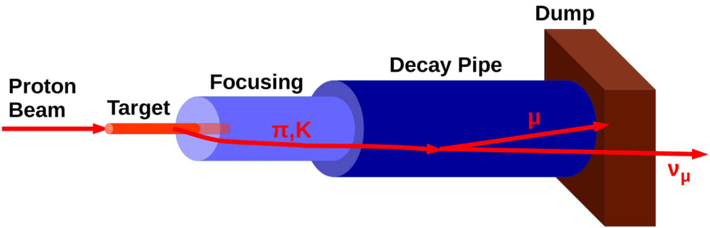

[DLL19].

Rough estimate of the flux

- A 8 GeV proton beam hits a target at rest, producing multiple hadrons.
  $\rightarrow$ Simulation of proton - proton collisions with Pythia, to get $\pi^\pm$ and $\pi^\pm$ $K^\pm$.
- Positively charged particles are focused and negatively charged particles deflected.
  $\rightarrow$ Alignment of π^+ and K^+ with the beam direction, with 10% forward K^- and π^- contamination.
- Particles that survived the focusing horn decay in a hollow pipe.
  $\rightarrow$ Geometric cuts are applied to the daughter neutrinos.

Total flux

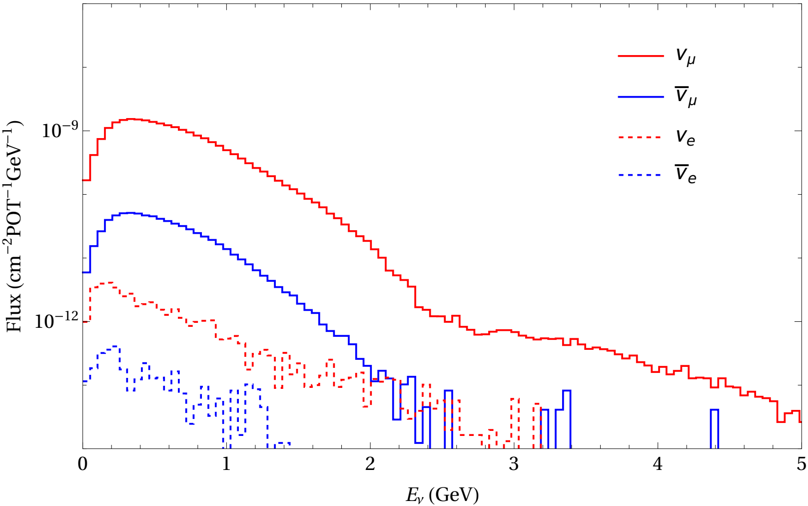

The estimated total neutrino flux at SBND.

Inner layer flux

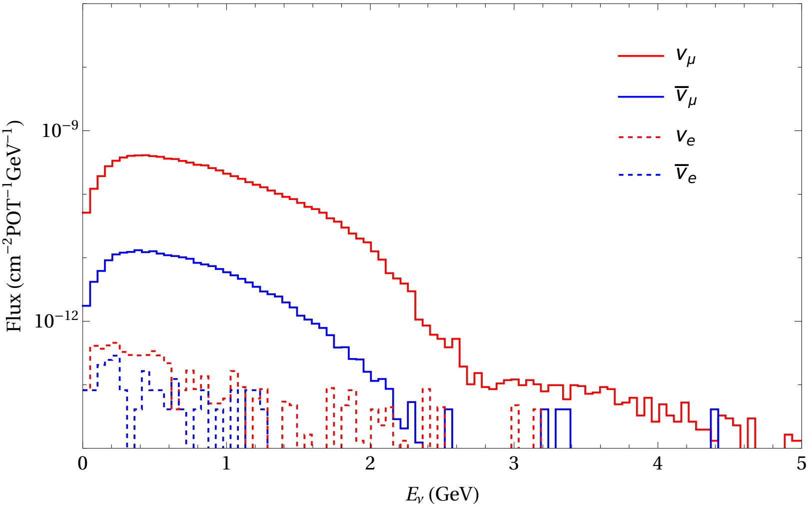

The estimated neutrino flux at PRISM inner layer, with distance $r < 1$ m from the beam axis.

Intermediate layer flux

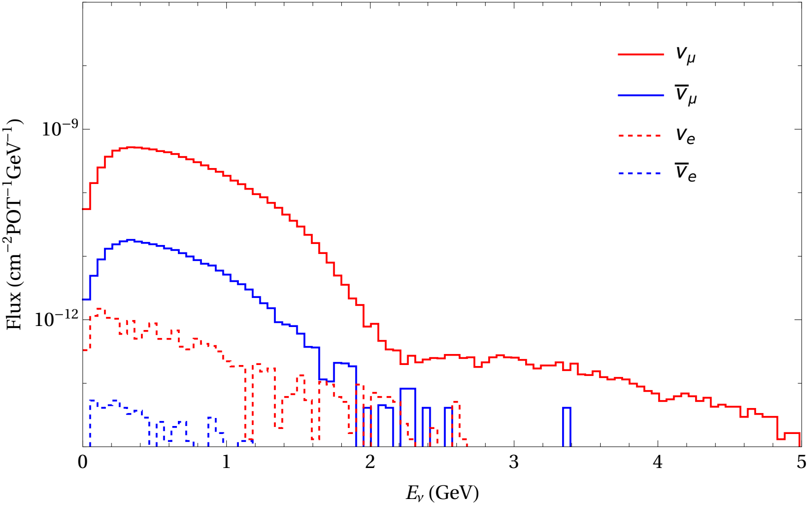

The estimated neutrino flux at PRISM intermediate layer, with distance 1 m $< r <$ 2 m from the beam axis.

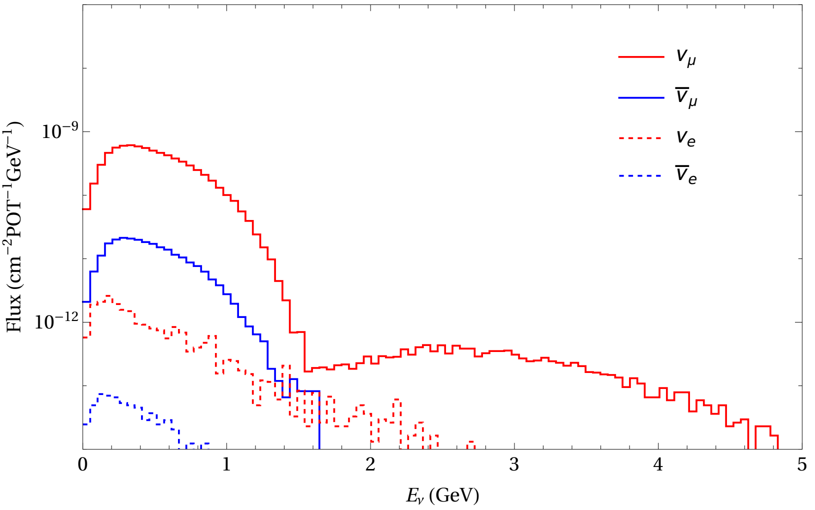

The estimated neutrino flux at PRISM outer layer, with distance 2 m $< r <$ 3 m from the beam axis..

The process we used to measure $\sin^2\theta_W$ is the elastic scattering of neutrinos off Argon atom's electrons:

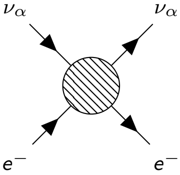

The process we used to measure $\sin^2\theta_W$ is the elastic scattering of neutrinos off Argon atom's electrons:

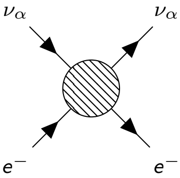

Signal events

So signal events are those that leave a single electromagnetic (EM) shower in the detector

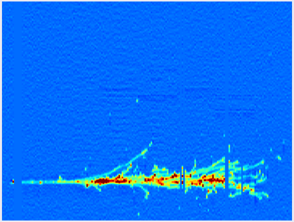

[A+20]

Background budget

Process at SBND

Table: SBND detector events simulation using the NuWro event generator [GSZ12].

Process	$\approx$ Fraction
Quasi elastic CC	47%
Quasi elastic NC	18%
Resonant CC	19%
Resonant NC	7%
Deep inelastic CC	0.9%
Deep inelastic NC	0.6%
Coherent CC	0.4%
Coherent NC	0.3%
Meson exchange CC	7%
Hyperon production	0.01%
Neutrino-electron scattering	0.006%

Compered to other processes, we have very few neutrino-electron scattering events!

Background budget

Process at SBND

Table: SBND detector events simulation using the NuWro event generator [GSZ12].

Process	≈ Fraction
Quasi elastic CC	47%
Quasi elastic NC	18%
Resonant CC	19%
Resonant NC	7%
Deep inelastic CC	0.9%
Deep inelastic NC	0.6%
Coherent CC	0.4%
Coherent NC	0.3%
Meson exchange CC	7%
Hyperon production	0.01%
Neutrino-electron scattering	0.006%

Compered to other processes, we have very few neutrino-electron scattering events!

- Events with hadronic activity can be discarded.

Background budget

Process at SBND

Table: SBND detector events simulation using the NuWro event generator [GSZ12].

Process	≈ Fraction
Quasi elastic CC	47%
Quasi elastic NC	18%
Resonant CC	19%
Resonant NC	7%
Deep inelastic CC	0.9%
Deep inelastic NC	0.6%
Coherent CC	0.4%
Coherent NC	0.3%
Meson exchange CC	7%
Hyperon production	0.01%
Neutrino-electron scattering	0.006%

Compered to other processes, we have very few neutrino-electron scattering events!

- Events with hadronic activity can be discarded.
- Events with multiple EM showers can be discarded.

Process at SBND

Table: SBND detector events simulation using the NuWro event generator [GSZ12].

Process	$\approx$ Fraction
Quasi elastic CC	47%
Quasi elastic NC	18%
Resonant CC	19%
Resonant NC	7%
Deep inelastic CC	0.9%
Deep inelastic NC	0.6%
Coherent CC	0.4%
Coherent NC	0.3%
Meson exchange CC	7%
Hyperon production	0.01%
Neutrino-electron scattering	0.006%

Compered to other processes, we have very few neutrino-electron scattering events!

- Events with hadronic activity can be discarded.
- Events with multiple EM showers can be discarded.
- We are left mainly with events containing a single visible photon coming from π^0 decay, but still giving a signal to background ratio of $\approx 1/4$.

Process at SBND

Table: SBND detector events simulation using the NuWro event generator [GSZ12].

Process	$\approx$ Fraction
Quasi elastic CC	47%
Quasi elastic NC	18%
Resonant CC	19%
Resonant NC	7%
Deep inelastic CC	0.9%
Deep inelastic NC	0.6%
Coherent CC	0.4%
Coherent NC	0.3%
Meson exchange CC	7%
Hyperon production	0.01%
Neutrino-electron scattering	0.006%

Compered to other processes, we have very few neutrino-electron scattering events!

- Events with hadronic activity can be discarded.
- Events with multiple EM showers can be discarded.
- We are left mainly with events containing a single visible photon coming from π^0 decay, but still giving a signal to background ratio of $\approx 1/4$.

We'll see shortly that a kinematic cut will remedy that issue.

Let's suppose that the only visible particle in an event is a π^0, and that it decays with a small angle relative to the beam direction in its rest frame...

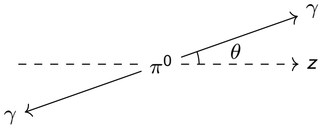

Typical background event

Let's suppose that the only visible particle in an event is a π^0, and that it decays with a small angle relative to the beam direction in its rest frame...

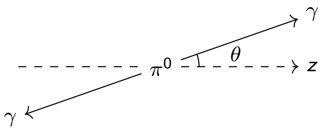

... it can result in a low energy invisible photon and a boosted visible photon in the rest frame: a single EM shower.

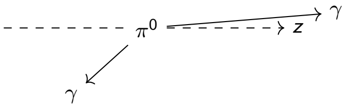

Let's suppose that the only visible particle in an event is a π^0, and that it decays with a small angle relative to the beam direction in its rest frame...

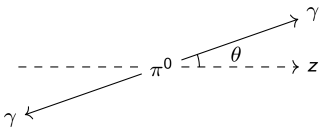

... it can result in a low energy invisible photon and a boosted visible photon in the rest frame: a single EM shower.

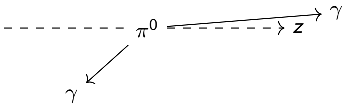

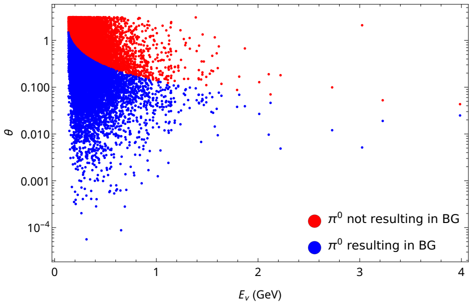

Still after all those events cuts, we still have much more background events than signal events.

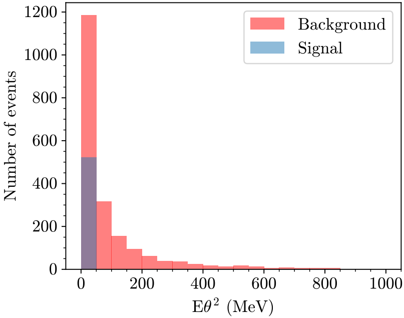

Still after all those events cuts, we still have much more background events than signal events.

But since $E_\nu \gg m_e$, we can use the ultra-relativistic, where for small angles we obtains

$$E\theta^2 < 2m_e\,.$$

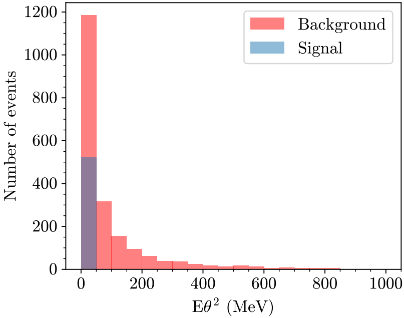

Still after all those events cuts, we still have much more background events than signal events.

But since $E_\nu \gg m_e$, we can use the ultra-relativistic, where for small angles we obtains

$$E\theta^2 < 2m_e\,.$$

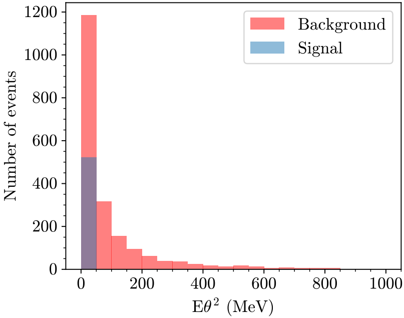

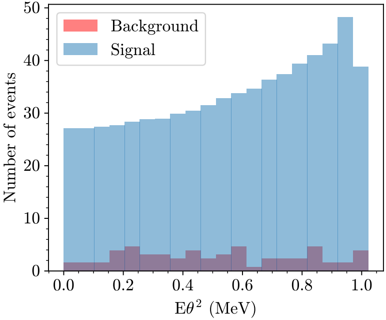

Statistics used

We used the following likelihood function for describing the counts at the detector:

$$\mathcal{L}(\sin^2\theta_W) = \frac{1}{N}\exp\left(-\frac{1}{2}\Delta^T\Sigma\Delta\right),$$

where $\Delta = N^{\text{pred}}(\sin^2\theta_W) - N^{\text{obs}}$, where N^{pred} is the predicted number of events and N^{obs} is a mock data set generated with the most recent global fit of $\sin^2\theta_W$.

Statistics used

We used the following likelihood function for describing the counts at the detector:

$$\mathcal{L}(\sin^2\theta_W) = \frac{1}{N}\exp\left(-\frac{1}{2}\Delta^T\Sigma\Delta\right) ,$$

where $\Delta = N^{\text{pred}}(\sin^2\theta_W) - N^{\text{obs}}$, where N^{pred} is the predicted number of events and N^{obs} is a mock data set generated with the most recent global fit of $\sin^2\theta_W$.

For the covariance matrix Σ, we used

$$\Sigma_{ij} = (\sigma_c^2 + \delta_{ij}\sigma_u^2)N_i^{\text{pred}}N_j^{\text{pred}} + \delta_{ij}N_j^{\text{pred}} , \quad \text{with} \quad \sigma_c = 10\% , \quad \sigma_u = 1\%, .$$

Statistics used

We used the following likelihood function for describing the counts at the detector:

$$\mathcal{L}(\sin^2\theta_W) = \frac{1}{N}\exp\left(-\frac{1}{2}\Delta^T\Sigma\Delta\right),$$

where $\Delta = N^{\text{pred}}(\sin^2\theta_W) - N^{\text{obs}}$, where N^{pred} is the predicted number of events and N^{obs} is a mock data set generated with the most recent global fit of $\sin^2\theta_W$.

For the covariance matrix Σ, we used

$$\Sigma_{ij} = (\sigma_c^2 + \delta_{ij}\sigma_u^2)N_i^{\text{pred}}N_j^{\text{pred}} + \delta_{ij}N_j^{\text{pred}}, \quad \text{with} \quad \sigma_c = 10\%, \quad \sigma_u = 1\%, .$$

This results in the χ^2

$$\chi^2 = \Delta^T\Sigma\Delta .$$

Using $\sigma_c = 10\%$.

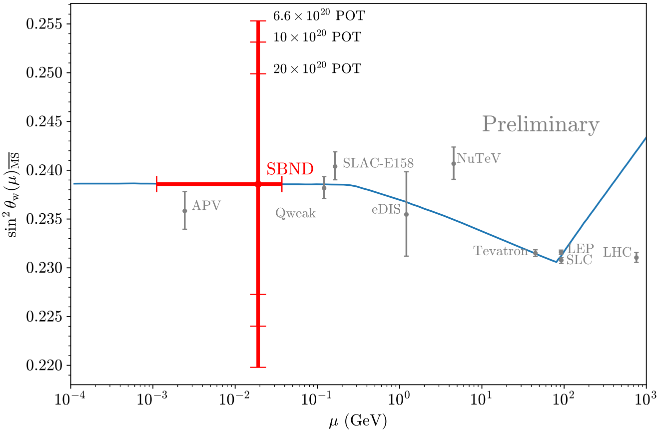

The addition of our SBND value for $\sin^2\theta_W$ to the running plot. The horizontal error bars correspond to the accessible scale $\mu = q$ accessible to the detector.

Using $\sigma_c = 5\%$.

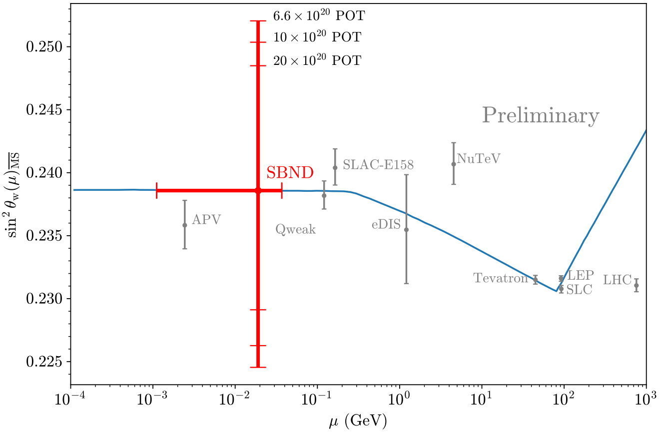

The addition of our SBND value for $\sin^2\theta_W$ to the running plot. The horizontal error bars correspond to the accessible scale $\mu = q$ accessible to the detector.

Conclusions

- Measurements of the weak mixing angle may give us precious insight to Standard Model and beyond Standard Model Physics, specially when performed in the neutrino sector.

Conclusions

- Measurements of the weak mixing angle may give us precious insight to Standard Model and beyond Standard Model Physics, specially when performed in the neutrino sector.
- A measurement of the weak mixing angle at SBND would fit nicely into the SBND physics program, contributing to the estimation of a flux measurement uncertainty and search for new new Physics.

Conclusions

- Measurements of the weak mixing angle may give us precious insight to Standard Model and beyond Standard Model Physics, specially when performed in the neutrino sector.
- A measurement of the weak mixing angle at SBND would fit nicely into the SBND physics program, contributing to the estimation of a flux measurement uncertainty and search for new new Physics.
- Analysis will be improved with the official SBND flux and covariance matrix.

Thank you for your kind attention!

C. Adams et al.
Deep neural network for pixel-level electromagnetic particle identification in the MicroBooNE liquid argon time projection chamber.
Phys. Rev. D, 99(9):092001, 2019.

R. Acciarri et al.
First measurement of electron neutrino scattering cross section on argon.
Phys. Rev. D, 102(1):011101, 2020.

John N. Bahcall, Marc Kamionkowski, and Alberto Sirlin.
Solar neutrinos: Radiative corrections in neutrino - electron scattering experiments.
Phys. Rev. D, 51:6146–6158, 1995.

Ubaldo Dore, Pier Loverre, and Lucio Ludovici.
History of accelerator neutrino beams.
Eur. Phys. J. H, 44(4-5):271–305, 2019.

A. Ferroglia, G. Ossola, and A. Sirlin.
The Electroweak form-factor kappa-hat (q**2) and the running of sin**2 theta-hat (W).
Eur. Phys. J. C, 34:165–171, 2004.

T. Golan, J. T. Sobczyk, and J. Zmuda.
NuWro: the Wroclaw Monte Carlo Generator of Neutrino Interactions.
Nucl. Phys. B Proc. Suppl., 229-232:499–499, 2012.

K. S. Kumar, Sonny Mantry, W. J. Marciano, and P. A. Souder.
Low Energy Measurements of the Weak Mixing Angle.
Ann. Rev. Nucl. Part. Sci., 63:237–267, 2013.

Omar G. Miranda, Guadalupe Moreno-Granados, and Celio A. Moura.
Sensitivity of accelerator-based neutrino experiments to neutrino-electron scattering radiative corrections.
Phys. Rev. D, 104(1):013007, 2021.

Pedro AN Machado, Ornella Palamara, and David W Schmitz.
The Short-Baseline Neutrino Program at Fermilab.
Ann. Rev. Nucl. Part. Sci., 69:363–387, 2019.

M. Tanabashi et al.
Review of Particle Physics.
Phys. Rev. D, 98(3):030001, 2018.

Marco Del Tutto and Vishvas Pandey.
Sbnd-prism.
In *NuSTEC CEWG Meeting*, June 3, 2021.

C. S. Wood, S. C. Bennett, D. Cho, B. P. Masterson, J. L. Roberts, C. E. Tanner, and Carl E. Wieman.
Measurement of parity nonconservation and an anapole moment in cesium.
Science, 275:1759–1763, 1997.